

‘Origami’ Horn Antenna for Contactless Vital Sign Monitoring

A Technical Report submitted to the Department of Biomedical Engineering

Presented to the Faculty of the School of Engineering and Applied Science
University of Virginia • Charlottesville, Virginia

In Partial Fulfillment of the Requirements for the Degree
Bachelor of Science, School of Engineering

Matthew T. Beyer

Spring, 2023

Technical Project Team Members

Matthew T. Beyer

Alec D. Figler

On my honor as a University Student, I have neither given nor received unauthorized aid on this assignment as defined by the Honor Guidelines for Thesis-Related Assignments

Dr. Shannon Barker, Department of Biomedical Engineering

'Origami' Horn Antenna for Contactless Vital Sign Monitoring

Matthew T. Beyer^a, Alec D. Figler^{a,1}, Dr. Kevin Owen^{b,c}

^a Department of Biomedical Engineering, University of Virginia

^b Raven Scientific, LLC.

^c Rivanna Medical, Inc.

¹ Correspondence: Email: alecfigler@gmail.com, Phone: (434) 882-8262

Abstract

Contactless cardiopulmonary detection offers promising applications in settings where conventional methods requiring contact cannot be used. For example, this detection could be used to monitor contagious patients without contact, or be used free from unplanned device removal. Chest displacements caused by respiration and cardiac activity can be radio detected, optimally by horn antennas, of which the flared geometry offers directivity and noise reduction, important for detecting subtle signal changes. However, commercially available horn antennas are expensive, reaching prices of \$2,000 for a single antenna. Furthermore, commercial manufacturers produce antennas of limited geometric variety, thus limiting potential application in research and product development. This capstone project aimed to create a program and accompanying UI that allows users to input desired antenna geometry, and have outputted the files of the proper format to be manufactured via 3D printing of flexible printed circuit board (PCB). Flex PCB is a durable, heat resistant, and flexible material that costs a fraction of that of materials commonly used to make these antennas, such as machined brass or aluminum. 2D PCB templates could be printed, folded and soldered to yield their usable 3D form. We then sought to evaluate the performance of the antennas in comparison to their commercially available analogs. Python was used to create the geometry-generating function and accompanying UI. A custom measurement system was constructed to characterize the flex PCB antennas' performance. The final product, with few notable limitations, allows users to create custom horn antennas that may not be commercially available at a fraction of the cost of commercially available products.

Keywords: Vital signs, contactless monitoring, horn antenna, radio detection, customizable antennas

Introduction

Significance

Vital signs, including respiratory rate and pulse rate, can offer clinicians extremely important information about a hospitalized patient, as changes can often be indicative of deteriorating health. For example, many arrhythmias, characterized by irregular pulse rates, are associated with an increased risk of blood clots which can dislodge and result in a stroke¹. Thus, given the ease at which this information can be acquired, it is not only convenient but also imperative in deciding next steps for patient care. Current methods of detecting and monitoring respiration and pulse rate range from use of simple instruments like a

stethoscope or more intricate devices like a pulse oximeter or various forms of bioimpedance sensors. However useful these devices may be, they all have limitations that can affect both the users and the patients themselves.

Limitations of Conventional Devices

Pulse oximeters are ubiquitous in modern hospitals, and can provide information such as pulse rate immediately upon contact and usually without calibration. They utilize two wavelengths of light, red and infrared, to measure rhythmic changes in light transmission as a result of alterations in arterial blood volume throughout the cardiac cycle². The light utilized by pulse oximeters is subject to absorption in the skin, notably by melanin in darker-

skinned patients. This absorption results in positive-bias and can cause darker-skinned patients to receive inaccurate data which can compromise the care they receive³. This creates equity concerns that require addressing to ensure all patients receive adequate care unconditionally. A shared limitation of conventional methods of cardiopulmonary monitoring is that they all require direct contact with the patient. This can be through user-dependent contact such as with a stethoscope, or contact of electrodes or photosensors such as with bioimpedance sensors and pulse oximeters, respectively. This contact can be suboptimal if a patient has a communicable disease, as the clinician would be at greater risk of contracting that disease with increased contact with the patient. There also exist instances where certain devices may not be viable as a result of damaged or destroyed tissue. Severe burning presents one of these instances by prohibiting proper electrode attachment or causing reduced circulation that could, for example, affect a pulse oximeter. Lastly, unplanned device removal can interfere with conventional devices. This is typically an issue with patients who are young children who might become uncomfortable, confused, or afraid and seek to remove devices in-use, which can pose a risk of harm, especially those who are critically ill⁴.

Innovation

These issues with potentially inaccurate measurement, as well as with limitations as a result of direct contact are evidence that contactless detection would benefit both clinicians and patients in a hospital setting. Radio detection is a promising candidate for this detection, as millimeter length radio waves are not affected by factors such as melanin, and allow for indirect assessment of a patient. Chest displacements as a result of respiration or cardiac contraction cause signal phase and amplitude changes that can be filtered and interpreted as either a heartbeat, inhalation, or exhalation. For example, with typical respiration rates being 10-20 breaths per minute, the respiration might be extracted at 0.1-0.3Hz, whereas pulse rate, averaging 60-100 beats per minute, might be extracted at 1Hz. For such subtle signal changes though, it is important to have minimal noise interference from the surrounding environment. Thus, a horn antenna is optimal due to its high gain and directivity which allow for transmission to and reception from specific directions, such as a patient.

Horn Antennas

Horn antennas are frustum, or apex-lacking pyramid, shaped antennas with high gain that produce a highly directive beam pattern. Gain refers to an antenna's ability to radiate in a specific direction, with higher gain meaning more angular directivity, and a narrower beam, and lower gain meaning less directivity and a wider beam. The radiation pattern of horn antennas produces a main “lobe” and periphery lobes of varying signal strength, however the point of highest signal strength for horn antennas is always directly in front of the antenna aperture, shown in Figure 1. The beam pattern is dependent on the antenna geometry, and largely determines what the antenna could be specifically used for. Currently, there are very few geometric varieties available commercially, and the ones that are available are very expensive, usually between \$1000-2000. This lack of variety and immense cost limits potential use in research and product development.

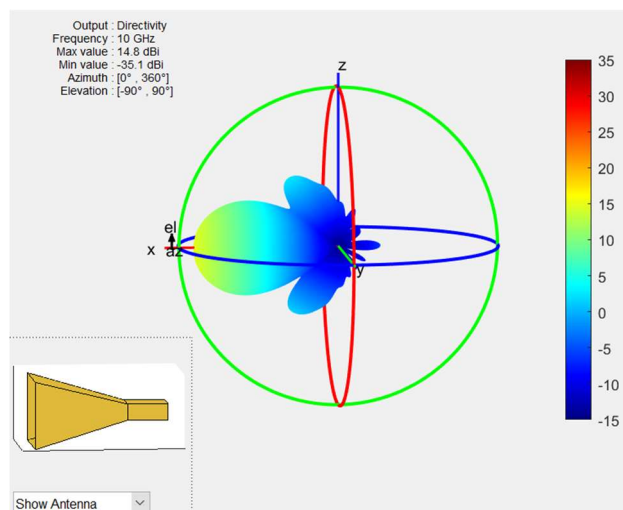


Figure 1. Example beam pattern of a horn antenna.

This figure shows how a typical horn antenna beam pattern behaves. The point of highest signal strength is directly in front of the aperture. Side lobe formation is also typical, as seen above. The area of primary interest is the lobe with the point of highest gain, or the “main lobe”. From Matlab’s Antenna Toolbox⁵

Project Aims

This project sought to solve the issues of limited geometry and high cost by creating a user interface that allows for generation of custom geometry, and utilizes a low-cost flexible PCB material, as opposed to the standard machined metal. The aim was to create a system that allows for fabrication of antennas that may not be commercially available and are user-specific at a fraction of the cost of commercial options.

Results

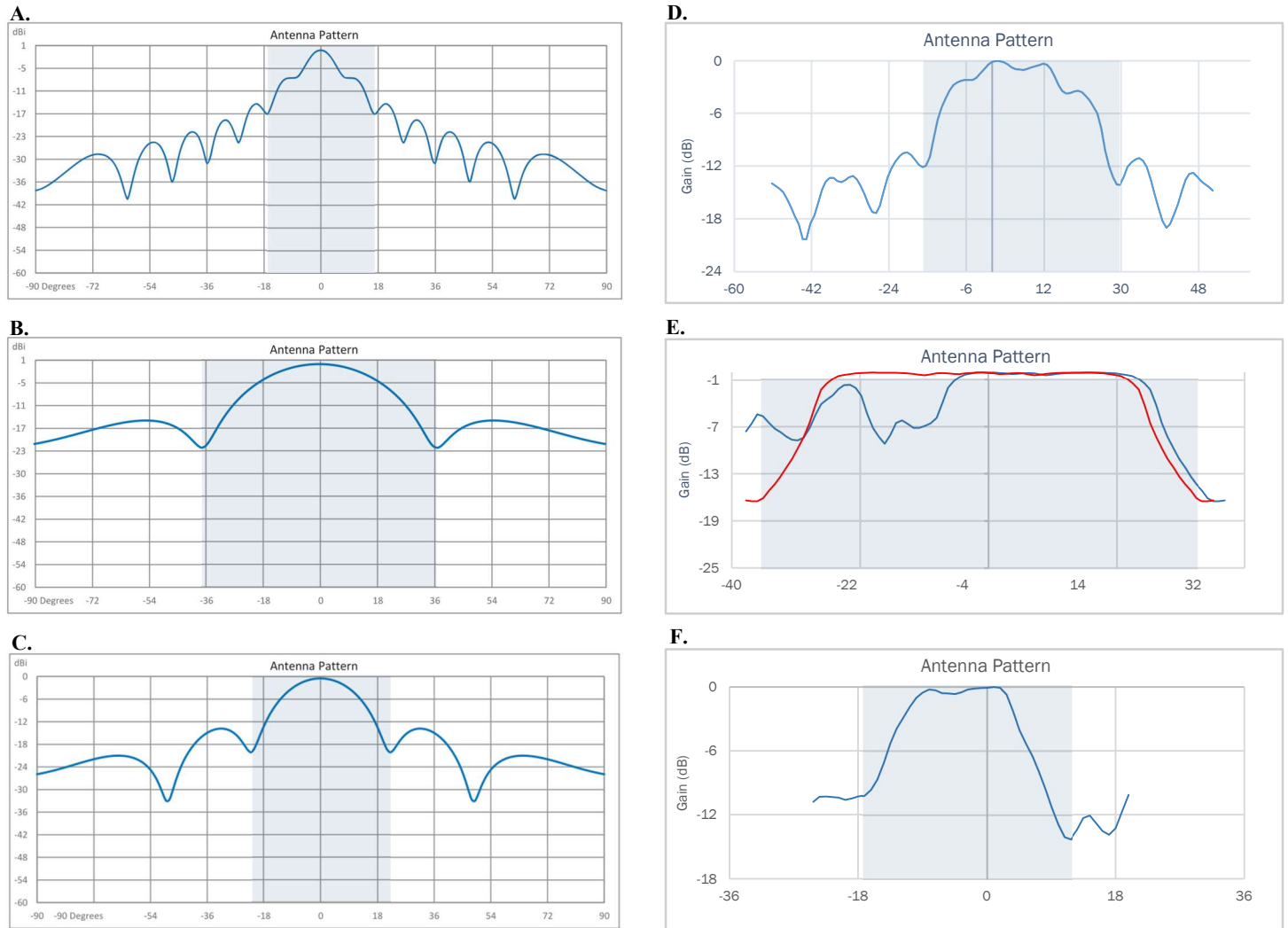


Figure 2. Beam Pattern Characterizations, with main lobe span indicated by the highlighted blue rectangles. (2A) Beam pattern characterization in the E plane for 20 dB calibration antenna, from Pasternack datasheet⁶. (2B) Beam pattern characterization in the E plane for 15 dB antenna, from Pasternack datasheet⁷. (2C) Beam pattern characterization in the E plane for 25 dB antenna, from Pasternack datasheet⁸. (2D) Beam pattern characterization from experimental measurement system for commercial 20 dB calibration antenna. (2E) Beam pattern characterization from experimental measurement system for 15 dB PCB antenna. (2F) Beam pattern characterization from experimental measurement system for 25 dB PCB antenna.

Antenna Performance

Calibration

The calibration of the measurement system, using a commercial 20 dB antenna, yielded a similar curve to that shown in the manufacturer datasheet, shown in Figure 2. Some signal splitting was observed, a limitation of the measurement system, but the lobes of the beam formed correctly, and the gain was roughly 20 dB, as expected. Primarily concerned with the angular response, this calibration gave the confidence in the measurement system to proceed with experimental measurements.

15 dB Antenna

One artifact of note in this curve is the variation in the negative direction, caused by overlapping signals. This will be addressed within the discussion section. In the positive direction, the signal is not disturbed, and a true version of the curve was generated by reflecting it over the 0° line, or aperture center. This curve shows the main lobe spanning roughly 72° ($\pm 36^\circ$ from center), agreeing with the manufacturer's datasheet, shown in Figure 2.

25 dB Antenna

The main lobe of the 25 dB antenna was slightly narrower than that described in the manufacturer datasheet. We expected a main lobe spanning about 48° ($\pm 24^\circ$ from center), but observed a span of 32° ($\pm 16^\circ$ from center), shown in Figure 2. However, as this was the highest gain antenna, it has the narrowest main lobe produced, consistent with expectations. Possibilities for imperfect replication are described further in the discussion section.

UI and Script Performance

The script successfully generates user-specified geometry for all the layers required, with few limitations to be discussed. The UI performs as needed to prompt users for the required arguments to call the function, and displays the generated geometry via a rendering of the Gerber template file, shown in Figure 3.

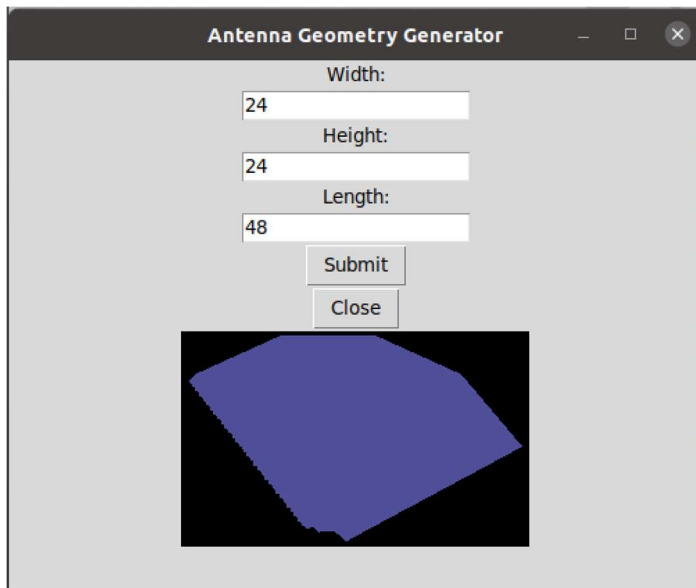


Figure 3. Example of UI parameter entry and output.

This is an example of parameter entry in the UI. The Gerber file is created and saved automatically, and a rendering is shown in the prompt window.

Discussion

Antenna Performance

Measurement System Performance

Generally speaking, the measurement system performed well in visualizing the beam pattern of an antenna. Although, there were notable limitations due to both the environment and setup itself. One limitation, visible in the characterization of the 15 dB antenna, is that the angled configuration of the transmitting and receiving antennas

allows for both reflected and direct signals to be received. Radio waves, a form of light, produce virtual images the same way a mirror will for visible light. In this setup, the identical virtual image of the transmission was being measured. The 15 dB antenna, having the lowest gain and therefore the widest main lobe, at a point in the negative direction was directly transmitting to the receiver, in addition to the desired reflected signal. This overlapping signal caused inaccurate power output values and thus a distorted curve, not representative of the true beam pattern. Fortunately, the direct transmission was not interfering in the positive direction, so the true curve was inferred from those measurements. Additionally, the environment in which measurements were taken was not free of reflective surfaces or other signal sources, so there was noticeably high background noise during measurements. Typically, antenna performance is measured in an anechoic chamber, which prohibits reflection of electromagnetic waves as well as outside sources from entering. However, these chambers are extremely expensive to build, and either renting one or shipping an antenna for measurement can cost hundreds of dollars.

Beam Pattern Analysis

The primary concern is that the angular response of the replicated antennas is similar to that of the performance described by the commercial manufacturer's datasheets. For a first iteration, the curves generated using PCB antennas closely match those of the commercial, metal antenna. This verifies that, for possible future iterations of this work, the folded-assembly PCB template is a viable alternative to the current commercial standard. The 15 dB antenna, with the exception of the limitations of the measurement system, produced the most similar results. The 25 dB antenna produced a slightly narrower beam, possibly as a result of imperfect replication of geometry or errors in assembly. However, with more precise assembly, flex PCB offers a promising alternative to more expensive commercial options.

Durability

The antennas are fragile, especially when the length is increased. A 20 dB antenna replicated broke during final experiments, representing the delicacy of the antennas and the way they are assembled. This demonstrates the need for a thicker PCB layer, as well as larger connecting tabs on the templates for more secure folding and soldering.

UI and Script Performance

The script that generates geometry performs as intended, producing a fabrication-ready Gerber template with all required layers. The UI that allows users to enter the

arguments also performs as needed, and is currently in its simplest form. It prompts for three arguments, as required to generate an antenna, and then displays a rendering of the Gerber file. The decision to include this rendering came as a result of an issue with the generation of some templates. While trying to create a 12 dB antenna, the template overlapped itself in a way that would prevent fabrication, as seen in Figure 4, so this rendering could quickly show users if they have valid geometry. A future solution to this problem might be having different template options, or multiple-component antennas to account for a more diverse array of geometry.

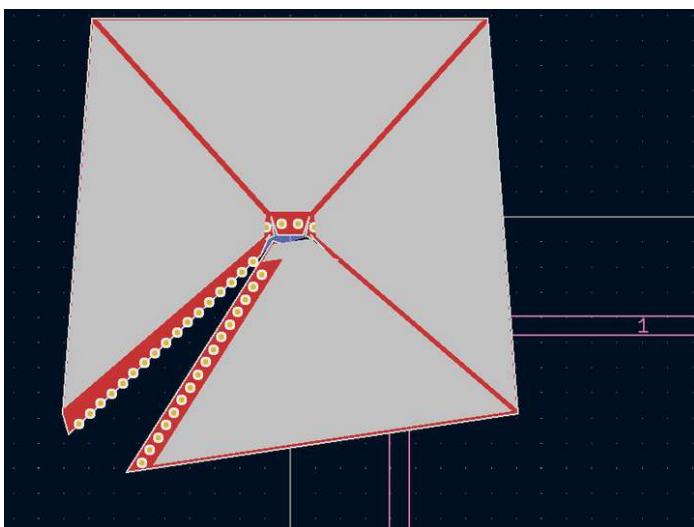


Figure 4. Invalid geometry of a planned 12 dB antenna. This figure shows an example of invalid geometry, with the template overlapping itself, making it incompatible with fabrication techniques. This was the output for an attempt at creating a 12 dB PCB antenna

Cost Comparison

One of the most significant results of this work was the reduction in cost from standard commercial prices. The selected fabricator, PCBWay, receives batch orders that are filled using sheets of flex PCB. The larger the batch ordered is, the cheaper each individual unit, or antenna, is. Exact pricing varies depending on quantity ordered or fabricator used, but the antennas fabricated for this project cost approximately \$5 per unit. This represents a tremendous reduction in cost, as, for reference, the 15 dB antenna replicated is commercially available for \$1,640. We were also able to get a quote from PCBWay for \$157 for 100 units, excluding shipping and additional fees. For researchers, this price difference could allow for construction of large arrays without massive losses in grant money. For a private company trying to market a device, this price reduction could mean the difference between whether or not a device will actually make it to market. In

general, with future iterations, this technology would become much more accessible for research and product development than it currently is.

Conclusion

We were able to create a significantly lower cost version of commercially available products and also demonstrated the ability to create novel antennas that may not be commercially available. As there are few, if any, services for designing custom antennas, this work demonstrates novelty in that regard. This customizable feature, in addition to the reductions in cost, improve the overall accessibility of this technology, aiming to increase its prevalence in research and medical device development. Future iterations of this work could involve strengthening the final product, adding more features to the UI, and possibly changing the arguments received by the UI. It can be difficult to determine what geometry is required to produce a certain beam pattern, so in the future, the arguments could be the desired gain and beam pattern, and then the function optimizes geometry to use as little material as possible to produce that. For a first iteration, this work showed promising signs that low-cost flex PCB could be an alternative material for horn antennas used in research and medical device development.

Materials and Methods

User Interface

A UI was constructed within the python program `gui.py`. Using the python source package `Tkinter`, `gui.py`⁹ displays a user interface to prompt users for desired height, width, and length of the antenna. These parameters are then provided through a subprocess to another user-created program, `antenna.py`, which takes the parameters and runs them through complex geometric formulas to determine the layered geometry necessary to print a flat version of a horn with the specified dimensions. Next, the `antenna.py` program uses a series of local functions create a Kicad file called `antenna.kicad_pcb`. At this point, the `gui.py` program uses the python package `pcbnew` to convert the `antenna.kicad_pcb` file to a Gerber file called `antenna.gbr`. A subprocess converts this `antenna.gbr` file to a `.png` file which is then displayed on the user interface to ensure that the generated geometry is as intended for the user. The output `antenna.gbr` file is then ready to be sent to a fabrication company. An example of this file is shown in Figure S1. A flow chart of this process is shown in Figure 5.

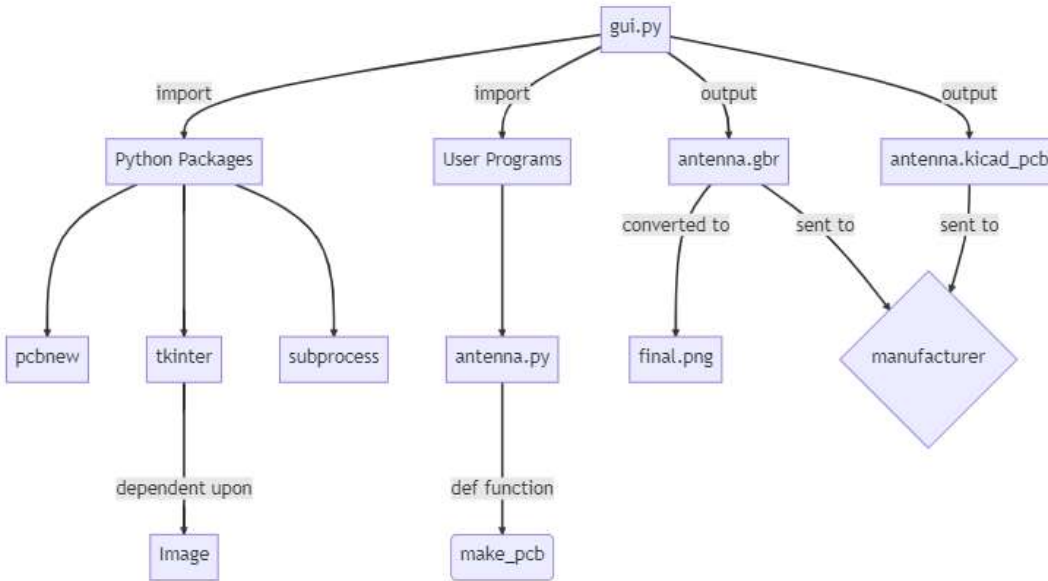


Figure 5. Flow chart of UI and geometry generating python function.

The process begins at the UI that prompts users for necessary arguments. Once received, the script that generates geometry is called and produces the PCB file required for fabrication. This PCB file proceeds through sub processing that creates a .png image rendering of the grebe file. The toolkit Tkinter generates the UI window, while the packages pcbnew and gerbrender are used to convert the gerber PCB file into an image format that can be displayed in the interface window. Following the dimension inputs, the outputs are the fabrication ready PCB file, as well as its image displayed in the prompt window.

Antenna Performance

Fabrication

Gerber PCB files of the desired geometry were generated with the geometry generating script and proofread for fabrication. These files were delivered to PCBWay, a Chinese fabricator, and put in queue for fabrication. The antennas were shipped from PCBWay in their 2D form. We then folded and soldered the antennas to yield their final, usable 3D form. The geometry of three antennas were replicated using the dimensions from CAD drawings within the manufacturer’s datasheet. The antennas replicated using PCB were a 15 dB and 25 dB antenna from Pasternack. The final, assembled products are shown in Figure 6. Pre folded templates are shown in Figure S2.

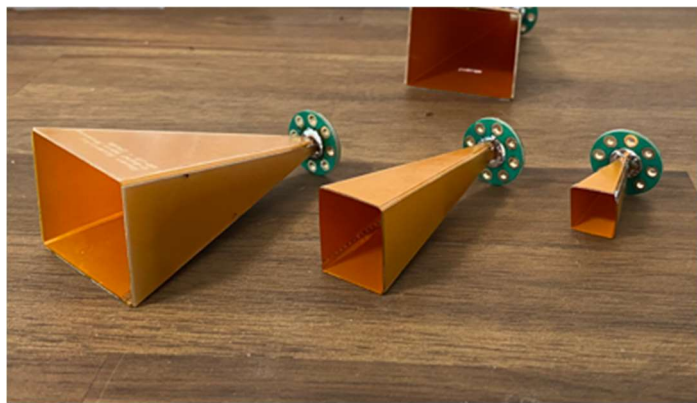


Figure 6. PCB antennas folded and soldered. From left to right, the PCB antennas are 20 dB, 25 dB, and 15 dB. Dimensions were copied from Pasternack datasheets, and represent an accurate replication of the commercial geometry.

Characterizing Beam Patterns

The measurement system constructed followed a standard antenna test lab configuration. The system utilized a step motor to rotate a base upon which experimental antennas were mounted, allowing them to rotate about the center of their apertures. This base was also raised approximately three feet from the ground to minimize interference from reflected signals. A diagram of this system is shown below in Figure 7.

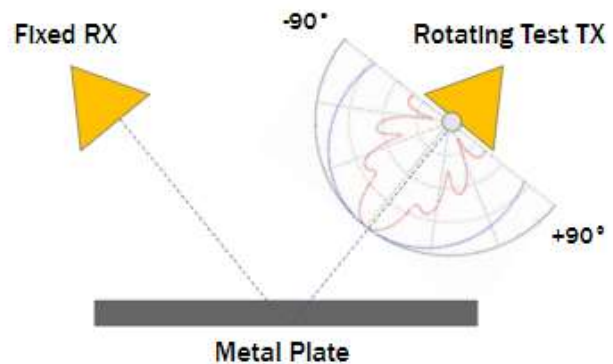


Figure 7. Diagram of Measurement System This figure shows a diagram of the measurement setup. The fixed receiver (RX) is a commercial antenna, while the transmitter (TX) is the interchangeable mount for the experimental antennas. Antennas were rotated about their aperture center via a step motor to sweep the beam pattern area of interest through the receiver range.

True pictures of the measurement system receiver and transmitter components are shown in Figure S3 and S4, respectively. The step motor was set to operate at 400 steps per rotation, or 0.9° per step. This rotation allowed for measurement of the angular response of the receiver to changes in directivity of test antenna transmission. The base was primarily made of wood and PVC components, with a number of custom 3D printed pieces to act as adapters. One 3D printed piece was created to support the waveguide, as it had a tendency to angle downwards as a result of the weight of the antennas. The experimental antennas were fixed atop the base, and its transmission “swept” through the receiver range, from the negative direction (from center) to the positive direction. The receiver was mounted atop a tripod with its aperture center at the exact height of the experimental antenna’s. This allowed the “lobes” of the antenna’s beam pattern to be plotted and the angular response observed. The three-dimensional pattern was measured in the two-dimensional elevational plane, as this is the standard convention for displaying antenna performance.

Increase of Effective Range

Initially, the transmitting and receiving antennas were facing directly at each other separated by 1 meter, however this caused the power output on the receiving end to reach a maximum, as the signal strength was too strong. For this reason, both antennas were aimed at a metal plate to reflect the signal, increasing the effective range. Each antenna was pointed at the center of the plate, distanced 1.5 meters from the center, forming a right angle, and creating an effective distance of about 3 meters. The power output is reduced by a factor of the distance squared, so the power output was reduced by a factor of 9, allowing for reduced power output that did not cause the receiver to reach maximum output.

Data Collection

Power output was measured at the receiver in volts, and this metric was converted to decibels using Equation 1¹⁰. This allowed for the generation of gain versus angular change plots.

$$\text{Equation 1: } A_p = 10 * \log_{10} \left(\frac{P}{P_{max}} \right) \text{ Decibels}$$

Calibration

To ensure that our system performed well, we sought to measure the angular response of a commercially available 20 dB antenna to evaluate how similar it is to the laboratory-measured performance shown in the commercial datasheet. This antenna was characterized

using the same method to characterize the experimental PCB antennas.

End Matter

Author Contributions and Notes

All authors contributed to designing the measurement system and using it to characterize the antennas. Matthew Beyer and Alec Figler performed work for the user interface. Dr. Kevin Owen wrote the code that generates the antenna geometry.

The authors declare no conflict of interest.

Acknowledgments

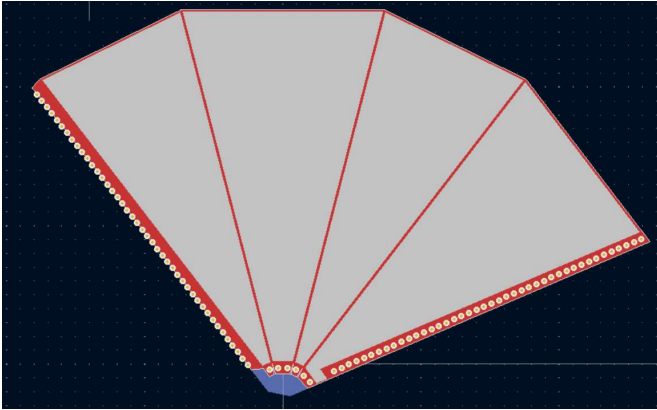
We would like to thank our advisor, Dr. Kevin Owen, for the funding, guidance, and preliminary work for this project.

References

1. Arrhythmia. National Heart, Lung, and Blood Institute. <https://www.nhlbi.nih.gov/health-topics/arrhythmia>. Accessed May 7, 2023.
2. Baura, G. *Medical Device Technologies: A Systems Based Overview Using Engineering Standards, Second Edition*. (Elsevier, Amsterdam, Netherlands)
3. Cabanas AM, Fuentes-Guajardo M, Latorre K, *et al.*. Skin pigmentation influence on pulse oximetry accuracy: a systematic review and bibliometric analysis. *Sensors*. 2022;22(9):3402. - <https://www.ncbi.nlm.nih.gov/pmc/articles/PMC9102088/>
4. Balmforth JE, Thomas AN. Unplanned Removal of Medical Devices in Critical Care Units in North West England Between 2011 and 2016. *Am J Crit Care*. 2019 May;28(3):213-221. doi: 10.4037/ajcc2019961. PMID: 31043401.
5. MathWorks, (2019). *Antenna Toolbox (R2019a)*. <https://www.mathworks.com/products/antenna.html>
6. WR-15 Waveguide Standard Gain Horn Antenna Operating from 50 GHz to 75 GHz with a Nominal 15 dBi Gain with UG-385/U-Mod Round Cover Flange. PEWAN1010, REV 1.0, Pasternack (2019). [Online] Available: <https://www.pasternack.com/images/ProductPDF/PEWAN1010.pdf>
7. WR-10 Waveguide Standard Gain Horn Antenna Operating from 50 GHz to 75 GHz with a Nominal 20 dBi Gain with UG-387/U-Mod Round Cover Flange. PEWAN1020, REV 1.0, Pasternack (2019). [Online] Available: <https://www.pasternack.com/images/ProductPDF/PEWAN1020.pdf>
8. WR-12 Waveguide Standard Gain Horn Antenna Operating from 60 GHz to 90 GHz with a Nominal 25 dBi Gain with UG-

- 387/U-Mod Round Cover Flange. PEWAN1015, REV 1.0, Pasternack (2019). [Online] Available: <https://www.pasternack.com/images/ProductPDF/PEWAN1015.pdf>
9. *Tkinter - Python interface to TCL/TK*. Python documentation. (2023). Retrieved May 7th, 2023, from <https://docs.python.org/3/library/tkinter.html>
 10. Decibels. Electronics Tutorials. <https://www.electronicstutorials.ws/filter/decibels.html>. Accessed May 7, 2023
 11. PCBWay – PCBWay, Hangzhou, China

Supplemental Material



Supplementary Figure 1 – Example output of Fabrication Ready PCB File.

This is an example of the PCB file output, complete with all layers required for fabrication and assembly including the PCB layer, copper layer, soldering mask, and castellations for soldering.



Supplementary Figure 2 – Unfolded antenna templates.

This is how the unfolded, 2D antenna templates are shipped from the fabricator.



Supplementary Figure 3 – Receiver mounted on tripod

This is the actual receiver setup, represented by “Fixed RX” in Figure 7, mounted on a tripod to match the height of the transmitter.



Supplementary Figure 4 – Transmitter on custom rotating base.

This is the actual transmitter setup, represented by “Test TX” in Figure 7. The step motor is beneath the wooden frame and rotates the PVC stand atop which the actual test antennas are mounted. This is at equal height to the receiver tripod in Figure S3.